VOL. 11, NO. 12, JUNE 2016 ISSN 1819-6608
ARPN Journal of Engineering and Applied Sciences

www.arpnjournals.com

A SIMULATION OF FRICTION BEHAVIOR ON OXIDISED HIGH SPEED STEEL (HSS) WORK ROLLS

Wan Fathul Hakim W. Zamri[1], B. Kosasih[2], K. Tieu[2], Wan Aizon Wan Ghopa[1], M. Faiz Md Din[3], Ahmad Muhammad Aziz[1] and Siti Fatimah Hassan[1]
[1]Department of Mechanical and Materials, Faculty of Engineering and Built Environment, Universiti Kebangsaan Malaysia, Malaysia
[2]Faculty of Engineering, University of Wollongong, Australia
[3]Faculty of Engineering, Universiti Pertahanan Nasional Malaysia, Malaysia
E-Mail: fathul@eng.ukm.my

ABSTRACT

In this paper, a combined FE simulation and scratch experiments approach was used to simulate the contact established between a high-speed steel (HSS) work roll and a hot strip material in hot rolling, in which the top layer and the substrate represented the HSS roll and the tip of the indenter represented a particle from oxide scale formed on the strip steel. This work focused on the contact behaviour of the oxide scale in the roll bite during hot rolling. The coefficient of friction during the simulation tests was recorded. It was found that the evolution of the coefficient of friction could be divided into two stages which are incubation period and stationary period. Associated with the evolution of the coefficient of friction, the deformation behaviour and the displacement at the cross section were characterised to study the tribological behaviour of oxide scale in contacts. The results indicated that the deformation and wear mechanism of oxide layer surface vary in different depths of penetration. At the penetration depth 2 µm, the oxide scale on the pin surface is significantly deformed. At the stage 3.2 µm and 4 µm, which the coefficient of friction is stable, the maximum von Mises are significantly higher than the yield stress of the oxide layer (σ_y = 7 GPa) so that high plastic deformation occurs.

Keywords: oxide layer, high speed steel, finite element method, wear, friction.

INTRODUCTION

Many researches have been conducted to investigate the mechanisms of hot roll wear during the rolling process. Garza-Montes-de-Oca and Rainforth (2009) studied the wear mechanism experienced by high speed steel (HSS) work roll under different environmental conditions. According to Garza-Montes-de-Oca and Rainforth (2009), the high wear rates under dry sliding conditions are associated with oxidation and plastic deformation (*e.g.* ploughing and abrasion). These results suggest that the combined wear mechanism of oxidation and abrasion of HSS rolls affect the characteristics and the wear behaviour of HSS work rolls during rolling process. The review clearly identified the need for research that focuses on a combination of abrasive factors and oxidation.

Despite there being numerous studies, most of them focussed on the oxidation mechanism only. For example, Molinari *et al.* (2000) studied the oxidation mechanisms of high speed steels and their correlation with the particular microstructure and chemical composition. Zhu *et al.* (2010) comprehensively studied the oxidation in high speed steel roll material by in-situ investigations. As the current published research is mainly concerned with the behaviour of oxidation, less attention was paid to the abrasive factor. Abrasion represents the scratching of asperities of strip oxide layers against the oxide layers of the work rolls.

In addition, there is also limited information from existing literatures regarding the modelling of oxide scale formed on the work rolls. The model of oxide scale on strip steel by Krzyzanowski and Rainforth (2010) consisted of three sub-layers, each having different mechanical properties. However, Krzyzanowski and Rainforth (2010) did not apply an oxide layer on the work roll in their model because they focused only on the strip. A small part of the studies contributed to the scale on the work roll. Therefore, the main aim of the modelling was to develop a finite element model with data that reflects properties that are more specific for a particular oxide scale under investigation. Many models describing the properties and behaviour of oxide scale on stock (strip) are available (Tang, 2006; Krzyzanowski and Rainforth, 2010) but only a limited number of researches concentrate on the oxide layer on the work roll. In fact, the research that studied the modelling of oxide scale on strip considered the work roll as having no oxide layer for simplification. Hence, a range of techniques have been developed, each providing a partial insight.

This paper discusses about an indenter scratching on the oxide layers/high speed steel substrate systemwhich simulate the contact established between a high-speed steel (HSS) work roll and a hot strip material in hot rolling. The computer based simulations coupled with experimental study are needed to predict the wear behavior of the oxide layers. To understand how the oxide layer deforms when scratched by an asperity, a three-dimensional (3D) finite element (FE) simulation was carried out.

Simulation method

The ductile behavior of the high speed steel (HSS) oxide layer was studied using scratch simulation of two-body system, i.e. between asperities and oxide layers. As there is no clear explanation of the behaviour and characteristics of the oxide layer on HSS, either brittle or ductile, selection of the adopted models in the FE simulation are based on the following arguments. First, the

oxide scale layer on HSS can be considered ductile based on the nanoindentation experimental results (Zamri *et al.* 2012; Zamri *et al.* 2013). This justification is based on the AFM images and the nanoindentation load-displacement curves. The AFM images show that no cracking occurred and the oxide layer deformed plastically during nanoindentation. In addition, hematite buckles and acts as a plastic oxide layer when compressive thermal stresses are applied (Garza-Montes-de-Oca *et al.*, 2011).

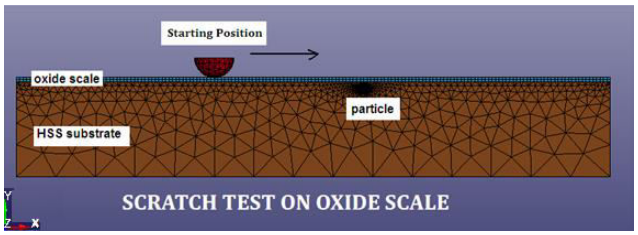

Figure-1. 3D FE model for simulating the scratch test: geometry and notation used.

The bi-linear model (ductile) was used to model the oxide layers where the eight-noded brick (oxide layer) and four-noded tetrahedral finite elements (substrate) with large strain and displacement capabilities, were used to discretise the target (Figure-1). The FE model for the specimen, shown in Figure-1, was 600 µm long, 100 µm wide and 100 µm thick, and that includes 4 µm for the thickness of the oxide layer. In view of their higher accuracy, brick elements were used in the impact region of the oxide layer, while the remaining substrate regions of the target were discretised using tetrahedral elements.

Table-1. Assumptions and parameters for FEM–based scratch test modelling for ductile model.

Oxide scale surface	**Ideally smooth**
Oxide scale/ Substrate interface	Perfectly bonded
Scratch distance (µm)	~200
Indenter tip radius(µm)	20
Oxide scale thickness(µm)	4
Oxide scale material	Fe_3O_4
Oxide scale material properties	E= 245 GPa, v= 0.2, σ_y= 7 GPa
Substrate material properties	E= 210 GPa, v= 0.3, σ_y= 2 GPa

The boundary conditions imposed on the above models were as follows: symmetry boundary conditions on the z = 0 and x = 0 planes, and the fully constrained workpiece bottom surface. The tip was treated as a rigid body and moved vertically and then horizontally into the oxide layer. The tip was kept reasonably low (12 m/min @ 200 µm/milliseconds) and it was assumed, for simplicity, that the temperature of the tip had a negligible influence on the material properties. The oxide layer was assumed to be perfectly bonded with the substrate where the oxide layer metal interface is relatively strong and allows no movement between the metal surface and the oxide layer. The assumption used in the FE modelling are summarised in Table-1.

The frictional contact problem of an indenter sliding on the surface of the Fe_3O_4 oxide scale/HSS substrate materials was analysed using Ansys-LSDyna Version 13. In addition, LS-PrePostVer 3.1 was used to export the data. After a convergence study, a suitable mesh density around the contact was found where the size of the elements was approximately half the thickness of the oxide layer. These dimensions were determined from numerous analyses to avoid establishing a boundary effect. Symmetric boundary conditions were applied to the central plane of the model. The model only considered one sub-layer due to the large 1:4 ratio of the outer sub-layer and inner sub-layer. For the ductile model, the material properties of the oxide layers and substrate were characterised by a bi-linear elastic–plastic model with isotropic hardening. The material deformed elastically when the stress applied was below the yield point (σ_y), but once the stress exceeded σ_y, the material deformed plastically with a strain hardening coefficient α. During plastic deformation the von Mises stress ($\sigma_{von\ Mises}$) is given by

$$\sigma_{von\ Mises} = \sigma_y + E_h \varepsilon_p \quad (1)$$

σ_y= yield strength
E_h= plastic hardening modulus
ε_p = plastic strain.
E_h is the plastic hardening modulus, $E_h = \alpha E$ (E is the Young's modulus)

The assumptions and parameters used in the FE modelling are summarised in Table-1. In order to validate the numerical model, the experimental result of the scratch test was compared with the experimental result of Zhou *et al.* (2008). The test conditionsand parameters used by Zhou *et al.* (2008) are listed in Table-2. In this study Zhou *et al.* (2008) studied the scratch behaviour of HSS for hot rolls using a Micro-scratch tester.

Figure-2 shows the comparison between the FE validation and Zhou *et al.* (2008) result of the apparent coefficient of friction versus the scratch length. The FE result had a good agreement with their result, but there were discrepancies during the running-in period. This was expected because the effect of local deformation is stronger at the initial stage, but then the coefficient of friction remains constant when the deformation and the pressure distributions are more uniform. The reason why the FE simulation showed the waviness at the initial stage is due to the effect of a rapid change in the contact force at the early operating stage (incubation period). In this work the average coefficient of friction was calculated from the second stage. A similar FEM observation was obtained with the previous study by Mezlini *et al.* (2005).

Table-2. The test conditions and parameters used by Zhou *et al.* (2008).

Type of load	Progressive load
Starting and end load (N)	0.05 / 25
Loading rate (N/min)	12.48
Scanning load (N)	0.05
Speed (mm/min)	0.5
Length (mm)	1

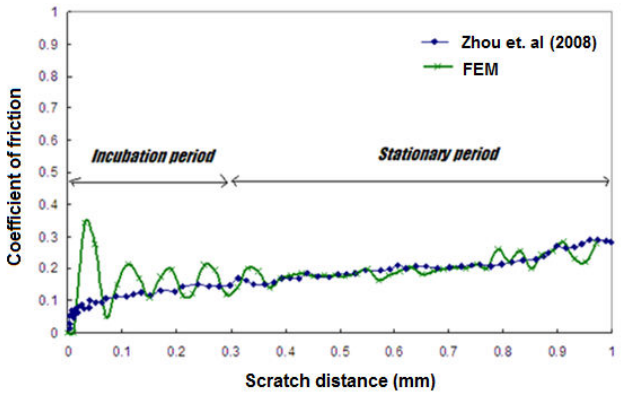

Figure-2. Comparison between developed FE model and experimental result of the coefficient of friction by Zhou *et al.* (2008).

Experimental and simulation results

The behavior of asperity scratching on the oxide layer has already been explored using scratch experiments. The significance of this study is due to the existence of abrasive phenomenon during the rolling process. It is important to understand the real size of asperities that can affect the wear of work roll. According to Sun *et al.* (2000) the diameters of the size surface imperfections at 10 and 20 s are close to 1.4 µm. In this case, an asperity can be considered as a particle from oxide scale formed on the strip surface. In the present work a 0.7 µm tip (diameter = 1.4 µm) was used in the scratch simulation to mimic the asperity sliding on oxide layer grown on work roll surface.

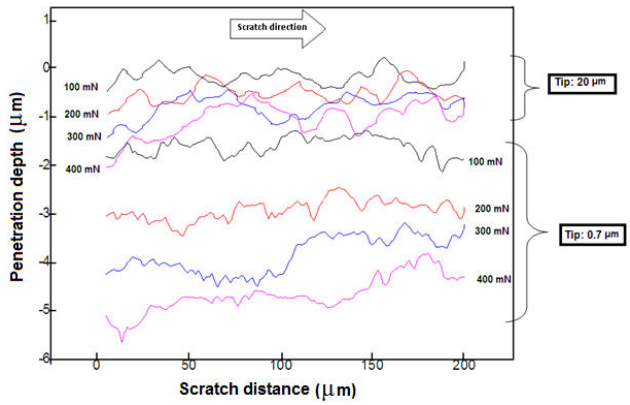

Figure-3. Variation of penetration depth of different tips for scratch test.

In order to investigate the effect of tip size on the depth of penetration a 20 µm tip was used as a comparison (Figure-3). The result shows that the depth of penetration by the 0.7 µm tip was at least twice as deep as with the 20 µm tip, and can actually penetrate the substrate in the real case of work rolls. In order to avoid the additional effect of the substrate during scratching, the 20 µm tip was applied in the following investigation on the behaviour of the oxide layer. Moreover, the behaviour of the scratch test would have been easier to investigate using numerical modelling if the larger tip was used.

The results of the evolution of the coefficient of friction by the 20 µm tip for a load of 100 mN, 200 mN, 300mN, and 400 mN are shown in Figure-4. Periodic changes in the coefficient of friction are clearly visible. This mode mimicked the wear testing of the material very well, and can therefore provide some insight into the wear behaviour of the material during scratching. With an increased load the magnitude of fluctuations in the coefficient of friction also increased because of the increased severity of the fractured regions on the oxide layer.

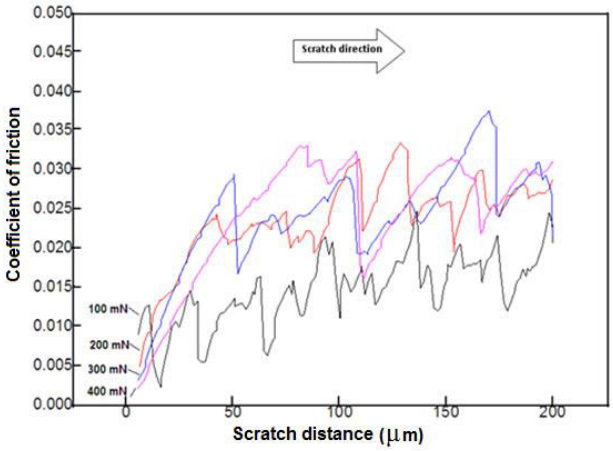

Figure-4. Evolution of the coefficient of friction of a 20 µm tip.

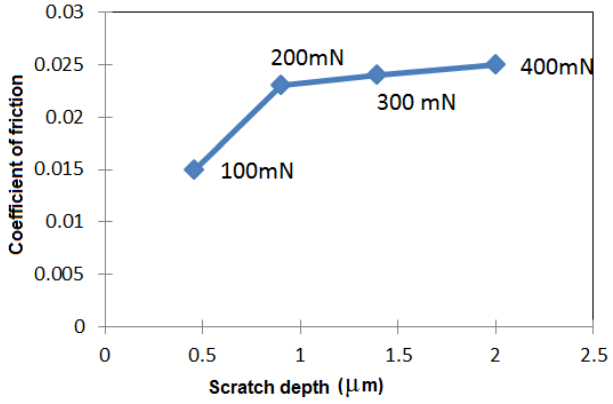

Figure-5. Variation of average coefficient of friction of a 20 µm tip as a function of the scratch depth.

The average coefficient of friction as a function of the depth by the 20 µm tip for a load of 100 mN, 200 mN, 300mN, and 400 mN are shown in Figure-5. The coefficient of friction increased in an approximately linear function with the depth of scratch due to saturation in ploughing of the oxide layer during scratching. As the indenter moves over the oxide layer, ploughing occurs during scratching and the ridges are formed on the sides of the track. When the scratching load is increased, deeper ploughing occurs due to increased load support and the indenter is pushed further into the material. As ploughing increases the friction there is a subsequent increase in the coefficient of friction, and the increased load also led to the formation of fractured surfaces consisting of micro-cavities.

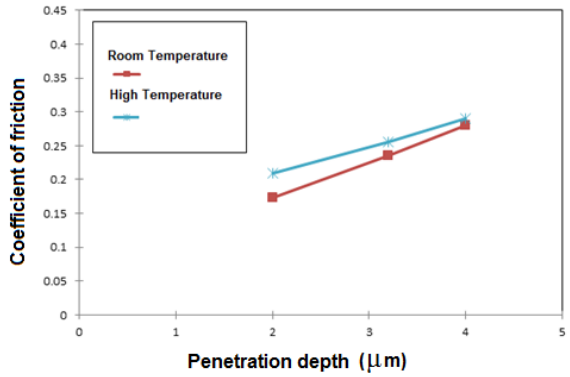

Figure-6. The variation of coefficient of friction as a function of scratch depth.

To simplify the modelling the scratch processes were simulated with constant applied depth mode. Figure 6 shows the variation in the coefficient of friction as a function of depth of scratch of 2 µm, 3.2 µm, and 4 µm for the ductile model at room and high temperature (600°C). The testing range between 2 - 4 µm of the penetration depth was selected based on the roughness of oxide scale on the strip that affects the work roll, which is around 1.44-3.13 µm, as reported by Sun (2005).

The coefficient of friction increases in an approximately linear function with the depth of scratch for both conditions, but is significantly higher under high temperature conditions because of the method of deformation and energy associated with the scratching process. The most drastic effect is when metal approaches the melting point so that the strength drops rapidly, and thermal diffusion and creep phenomena become more important. This increased adhesion at contacts and ductility lead to an increase in friction.

In addition, the coefficients of friction of the oxide scale for the ductile model at room temperature are slightly lower than at high temperature due to the mechanical properties where the hardness and Young's modulus (E) are higher at room temperatures which lead to better scratch resistance and lower coefficient of friction. This finding is consistent with the trend of the coefficients of friction reported by Garza-Montes-de-Oca and Rainforth (2009).

The results of comparing the coefficient of friction at a scratch depth of 2 µm with the experimental (Figure-5) and measured coefficients of friction (Figure-6) show that the measured coefficient of friction is marginally higher than experimental result at around 0.05 µm. This trend was probably due to the wide range of mechanical properties of oxide layers that lead to a discrepancy in the coefficient of friction. However, the coefficients of friction predicted by both models are consistent with the experimental works in terms of the increased trend where the coefficients of friction are correlated with the depth of penetration, as shown in Figure-5.

To further understand the results of the scratch simulation, the progressive stress field and deformation of the oxide layers at three stages are explained as illustrated in Figure-7. Three locations were considered, after indentation, at approximately half of the total scratch length, and at the final stage of scratch process.

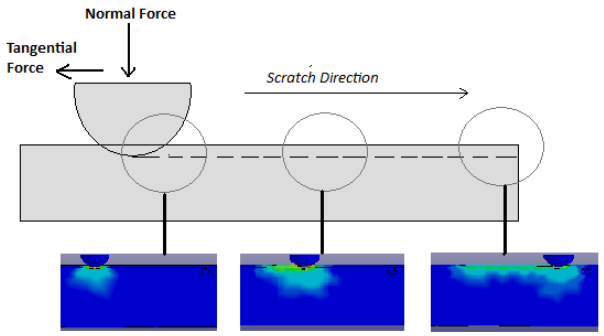

Figure-7. Deformation behavior during ductile regime nano-machining.

Figures-8(a) show the step of indentation into the oxide scale where there was no sliding movement, but only a normal load applied by the indenter. At a small depth of indentation plastic deformations occur around the tip of the indenter, which propagate vertically and laterally as a round shape. As the depth of penetration increases the plastic deformation propagates further under the surface and at the substrates. Plastic deformation also propagates vertically and laterally in the oxide layer and the substrate. Figures-8(b) show the middle stage of the scratching process (100 µm) where indenter slides on the surface under an applied normal depth and the material is ploughed. As the indenter moves the plastic deformation zone moves in the same direction and the plastic deformation zone has moved from the centre of the indenter towards the leading edge of the indenter, as shown in Figures-8(c).

Three scratch simulations were performed at three different depths, 4 µm, 3.2 µm, and 2 µmto observe how the depth of scratching deforms the oxide layer. The displacement controlled model was used to simulate the stress field when the same diamond tip slides over the oxide. The variations in compression and the tensional

stress field at the final stage (200 µm) of the scratch for three different depths are shown in Figure-9(a) to (c).

The compression and tensional stress field under the tip at 4 µm (Figure-9(a)) and 3.2 µm (Figure-9(b)) are around 14 GPa and 9 GPa respectively. The maximum von Mises for both cases is significantly higher than the yield stress of the oxide layer (σ_y = 7 GPa) so that high plastic deformation occurs. Meanwhile, the maximum von Mises at 2 µm is about 7 GPa. The maximum stress correlates with the scratch penetration where the maximum stress increases with the increases in the depth of penetration. This is because the maximum tensile strength and shear strength that reacted on the scratched surface - the main cause of the deformation - increased with the increased penetration of the tip.

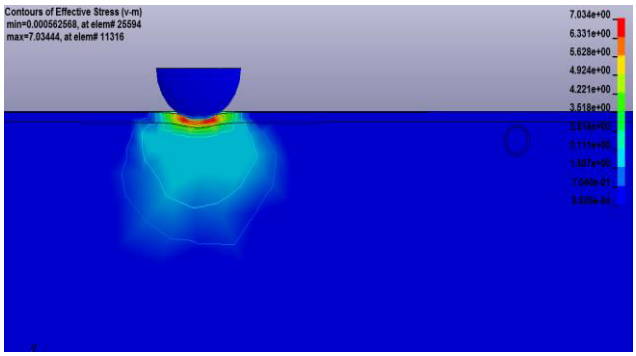

(a)

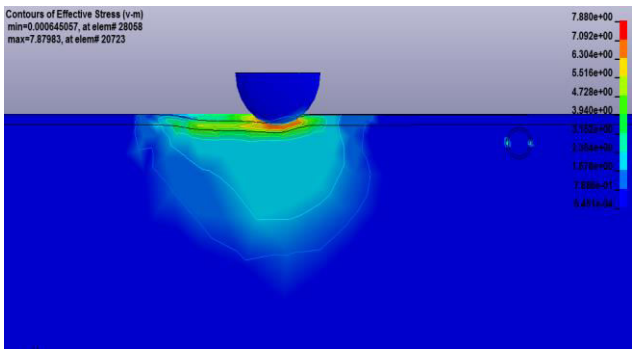

(b)

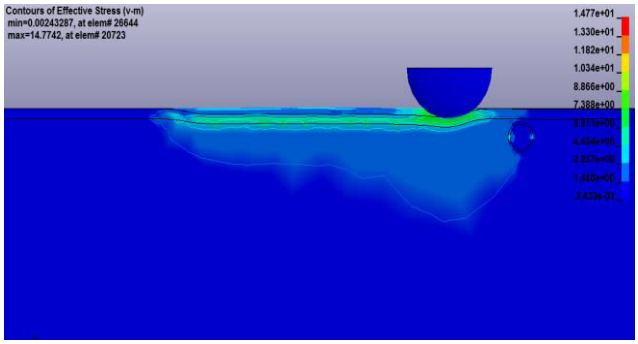

(c)

Figure-8. Development of a plastic zone in the scratch process (transverse section view): (a) loading process at 4 µm depth of penetration, (b) during scratch process (c) final stages.

The effect of the material characteristics is well illustrated in Figures-9(a) to (c) and they are related to the role of classic ploughing wear. This result also confirms the earlier observations by Garza-Montes-de-Oca *et al.* (2011) where the characteristics of the oxide layer on HSS might act as fairly plastic when compressive thermal stress is applied. For a more precise observation, the pile-up at the final stage (200 µm) was identified, as illustrated in Figure-10. The pile-ups that developed after the scratching tests at three different depths (4 µm, 3.2 µm and 2 µm) were investigated.

A pile-up is generated because most of the plastic deformation occurred near the tip of the diamond, and markedly occur for non-strain hardening materials with a larger value of elastic modulus (E) compared with that of the plastic strength (Y), E/Y (Youn and Kang, 2004). A half mild pile-up phenomenon occurred in the side of the model (Figure-10). The example cross sections of the post-profile displacement obtained by the scratch simulation tests are shown in Figure-10(b). This figure shows a very clean cross section and low pile-up that was due to the plastic zone being typically contained within the boundary of the circle of contact and the elastic deformation that accommodates the volume of indentation spreading further away from the indenter (Youn and Kang, 2004). Therefore, sink-in is more likely to occur in this case. All three cases (4 µm, 3.2 µm and 2 µm) have elastic recovery of around 0.4-0.7 µm.

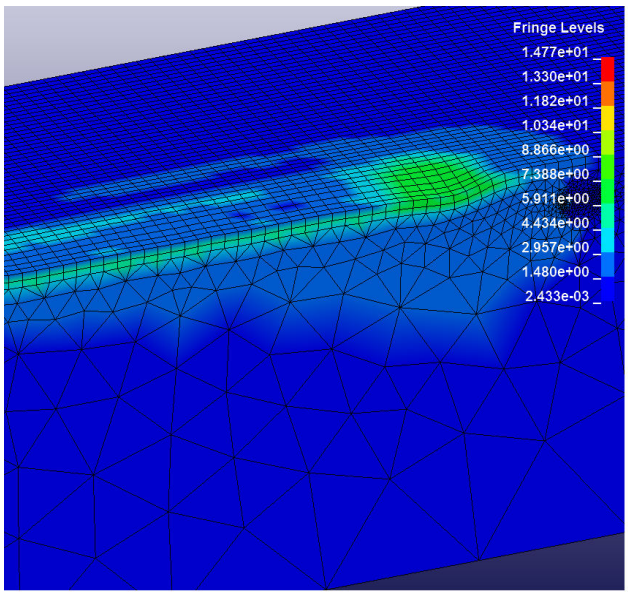

(a)

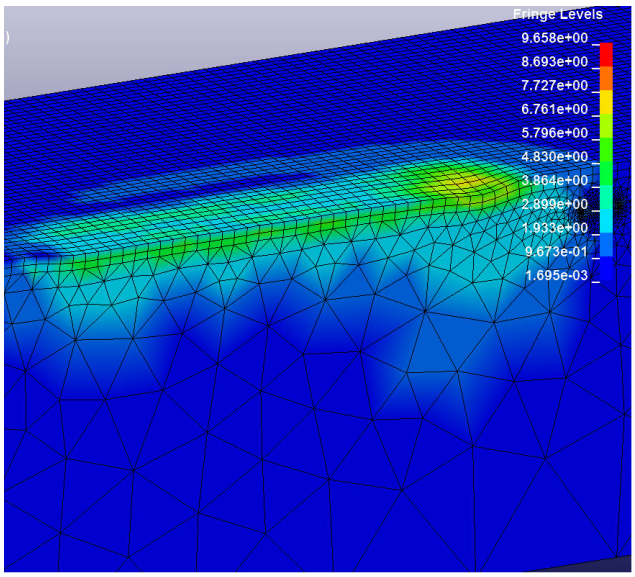

(b)

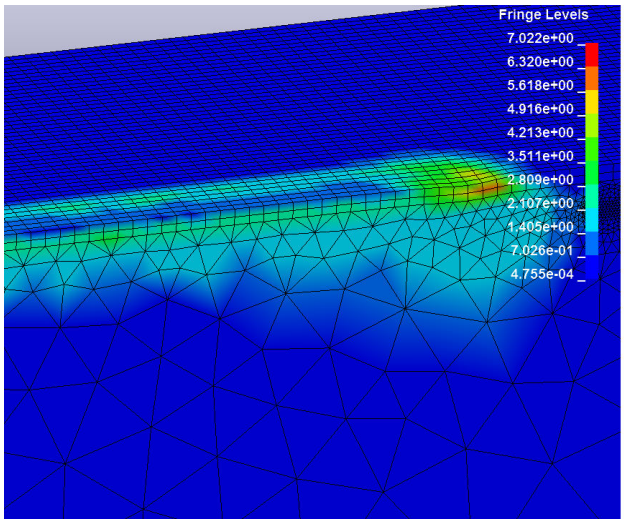

(c)

Figure-9. Stress field map showing von Mises stress on the oxide scale after scratch test. Sliding direction is from left to right and stress field at three different depths (a) 4 µm; (b) 3.2 µm; (c) 2 µm.

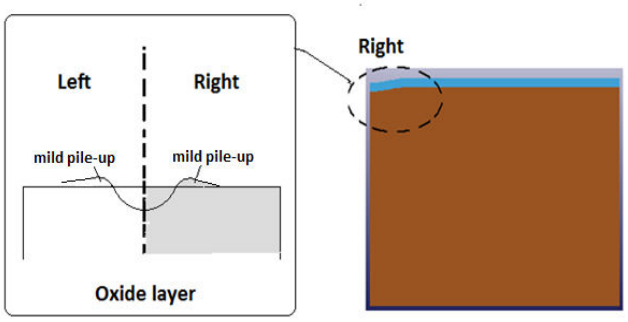

(a) (b)

Figure-10. The pile-up (a) the illustration of the pile-up (b) the region of pile-up.

Based on the pile-ups, the wears for three different cases were estimated using a profilometric study. The cross section study is often used to calculate the real wear area, A_w (Kato *et al.*, 1992), which also measures the difference between the grove area and the area at both sides (Figure-11).

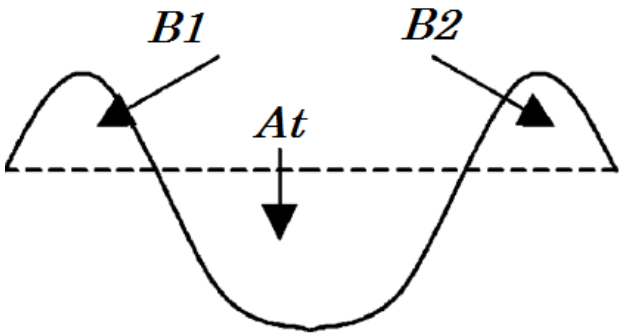

Figure-11. Definition of the degree of wear.

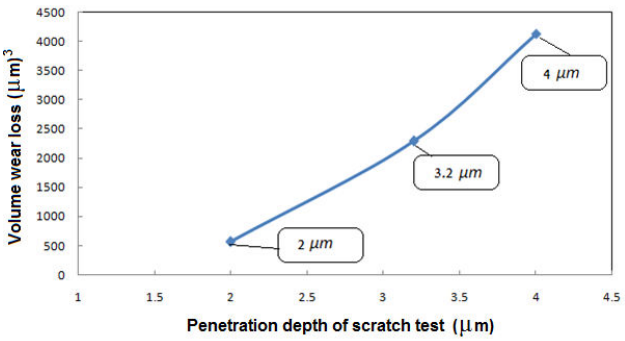

Figure-12. An estimation of the real wear volume for three different scratching depths.

Based on the result of the simulation, the real wear volume for length of scratch L = 200 µm at three different depths was estimated. The side ridges were very mild due to the creation of a frontal pile up that represents the ploughing mechanism. The trend of real wear volume is shown in Figure-12. As expected, the scratching at 4 µm provided the highest wear volume of 4140µm^3 followed by scratching at 3.2 µm (2290 µm^3) and 2 µm (564 µm^3). This scenario was due to the correlation between the wear and contact load (given by different depths of penetration). In other words the wear depends on the capability of the slider tip to penetrate into the oxide layer during sliding. The higher penetration means that more materials are removed.

CONCLUSIONS

A combined scratch tests and three-dimensional (3D) finite element (FE) simulation on oxide layers and high speed steel substrate system have been presented. Periodic changes in the coefficient of friction are clearly visible where the coefficient of friction increased because of the increased severity of the fractured regions on the oxide layer. The depth of penetration by the 0.7 µm tip

was at least twice as deep as with the 20 µm tip, and can actually penetrate the substrate in the real case of work rolls. The finite element result can be used to explain the scratch behaviour of oxide layer on high speed steel (HSS). The progressive stress field and deformation of the oxide layers at three stages are explained by the compression and tensional stress field. The maximum von Mises under the tip at 3.2 µm and 4 µm are significantly higher than the yield stress of the oxide layer (σ_y = 7 GPa) so that high plastic deformation occurs. The friction and scratch behaviour observed in the current study are probably related to the classical ploughing wear mechanism of oxide layers.

REFERENCES

Garza-Montes-de-Oca, N. F. and Rainforth, W. M. 2009. Wear mechanisms experienced by a work roll grade high speed steel under different environmental conditions. Wear, 267(1), pp. 441-448.

Garza-Montes-de-Oca, N. F., Colás, R. and Rainforth, W. M. 2011. Failure Modes of the Oxide Scale Formed on a Work Roll Grade High Speed Steel. Oxidation of metals, 76(3-4), pp. 149-160.

Kato, O., Yamamoto, H., Ataka, M. and Nakajima, K. 1992. Mechanisms of surface deterioration of roll for hot strip rolling. ISIJ international, 32(11), pp. 1216-1220.

Krzyzanowski, M. and Rainforth, W. M. 2010. Oxide scale modelling in hot rolling: assumptions, numerical techniques and examples of prediction. Iron making and Steelmaking, 37(4), pp. 276-282.

Molinari, A., Straffelini, G., Tomasi, A., Biggi, A. and Corbo, G. 2000. Oxidation behaviour of ledeburitic steels for hot rolls. Materials Science and Engineering: A, 280(2), pp. 255-262.

Sun, J. S., Lee, K. H. and Lee, H. P. 2000. Comparison of implicit and explicit finite element methods for dynamic problems. Journal of Materials Processing Technology, 105(1), pp. 110-118.

Tang, J., Tieu, A. K. and Jiang, Z. Y. 2006. Modelling of oxide scale surface roughness in hot metal forming. Journal of materials processing technology, 177(1), pp. 126-129.

Vergne, C., Boher, C., Gras, R. and Levaillant, C. 2006. Influence of oxides on friction in hot rolling: Experimental investigations and tribological modelling. Wear, 260 (9), pp. 957-975.

Youn, S.W. and Kang, C.G. 2004. A study of nanoscratch experiments of the silicon and borosilicate in air. Materials Science and Engineering A. pp. 384(1), pp. 275-283.

Zamri, W. F. H., Kosasih, P. B., Tieu, A. K., Zhu, Q. and Zhu, H. 2012. Variations in the microstructure and mechanical properties of the oxide layer on high speed steel hot rolling work rolls. Journal of Materials Processing Technology, 212(12), pp. 2597-2608.

Zamri, W. F. H, Kosasih, P. B., Tieu, A. K., Zhu, Q. and Zhu, H. 2013. Finite Element Modeling of the Nanoindentation of Layers of Porous Oxide on High Speed Steel, Steel Research International, 84(12), pp. 1309-1319.

Zhou, L., Sun, D., Liu, C., Li, C. and Yao, L. 2008. Scratch behavior of high speed steels for hot rolls. Journal of University of Science and Technology Beijing, Mineral, Metallurgy, Material, 15(4), pp. 402-406.

Zhu, Q., Zhu, H. T., Tieu, A. K., Reid, M. and Zhang, L. C. 2010. In-situ investigation of oxidation behaviour in high-speed steel roll material under dry and humid atmospheres. Corrosion Science, 52(8), pp. 2707-2715.